Excitation Temperature and Electron Number Density Measured for End-On-View Inductively Coupled Plasma Discharge

Sang-Ho Nam* and Young Jo Kim

The Department of Chemistry, College of Natural Sciences, Mokpo National University, 61, Dolim-Ri, Chungkye-myon, Muan-gun, Chonnam 534-729, Korea
Received April 16, 2001

The excitation temperature and electron number density have been measured for end-on-view ICP discharge. In this work, end-on-view ICP-AES equipped with the newly developed "optical plasma interface (OPI)" was used to eliminate or remove the negative effects caused by end-on-plasma source. The axial excitation temperature was measured using analyte (Fe I) emission line data obtained with end-on-view ICP-AES. The axial electron number density was calculated by Saha-Eggert ionization equilibrium theory. In the present study, the effects of forward power, nebulizer gas flow rate and the presence of Na on the excitation temperature and electron number density have been investigated. For sample introduction, two kinds of nebulizers (pneumatic and ultrasonic nebulizer) were utilized.

Keywords : Excitation temperature, Electron number density, ICP, end-on-view.

Introduction

ICP-AES (Inductively Coupled Plasma Atomic Emission Spectrometry) has been widely used for the determination of trace elements in various samples due to its high detection power, multi-elemental analysis, minor matrix and memory effect, high analysis speed and a tolerance to high salt concentration.[1,2] The main advantages result from the unique properties of ICP as atomization-ionization-excitation source for AES. The two of important properties of ICP discharge are temperature and electron number density.[3-6] The temperature of ICP discharge is important because the energy states and distribution of atoms, ions, and molecules can be greatly affected by temperature.[7-13] The electron number density is also critical because it can be used to estimate the degree of ionization of discharge. But, most measurements of temperature and electron number density[14-21] have been primarily done for the side-on-view ICP discharges. Thus, this work focuses on the measurement of temperature and electron number density of end-on-view ICP discharges. For the first time, the measurement for end-on-view ICP discharge was successfully achieved.

In the past, the atomization source of atomic emission spectrometry was mainly the side-on-view ICP discharges for radial observation. Recently, it has been found that detection limits of most elements could be improved with the end-on-view ICP discharges for axial observation of the plasma.[22-33] But it is also a fact that the end-on-view ICP discharges increase the matrix effect and spectral interference. In addition, the instability of the tailing of the plasma has been troublesome. Thus, in this work, end-on-view ICP-AES equipped with the newly developed "optical plasma interface (OPI)" has been used to eliminate or reduce the negative effects caused by the end-on-plasma source. The present work reports the excitation temperature and electron number density with end-on-view ICP-AES. The axial excitation temperature was measured using an analyte (Fe I) emission line data obtained with end-on-view ICP-AES.[3,4] The axial electron number density was calculated by Saha-Eggert ionization equilibrium theory.[3,4] In this study, the effect of the forward power, nebulizer gas flow rate and the presence of Na on excitation temperature and electron number density have been investigated. For sample introduction, two kinds of nebulizers (pneumatic and ultrasonic nebulizer) were utilized.

Experimental Section

Instrumentation. E-O-V ICP-AES (End-On-View Inductively Coupled Plasma Atomic Emission Spectrometer) equipped with the newly developed Optical Plasma Interface (OPI) was obtained from SPECTRO Analytical Instruments (SPECTRO A.I. GmbH Boschstr 10, D-47533 Kleeve, Germany). Details of the instrumental and operating conditions are described in Table 1. A schematic diagram of the Optical Plasma Interface (OPI) is shown in Figure 1. The radiation emitted by analytes enters the spectrometer through a concentric aperture. Argon flow in the opposite direction prevents the plasma from penetrating the aperture. The configuration helps eliminate any interference by a turbulent cross-jet which can affect the measurement precision and accuracy.

Chemicals and Reagents. All reagents were ICP-AES standards (VHG Labs, Inc., 180 Zachary Rd., Manchester, NH 03109, USA). Double distilled nitric acid was obtained from VHG Labs, Inc. Solutions were prepared in 2-5% nitric acid. All solutions also were prepared with 18 MΩ · cm distilled deionized water.

Measurement of Excitation Temperature (T_{exc}). Neutral atoms, ions, molecules, and electrons in plasma are distributed over many energy states. The distribution states depend on the temperature of the plasma. The excitation temperature

Table 1. Instrumental and Operation Condition

Plasma operating condition (for axial torch observation)	
R.F. power	: 1000-1500 W
R.F. frequency	: 27.12 MHz
Outer gas flow	: 14 L/min
Intermediate gas flow	: 1.7 L/min
Injector gas flow	: 0.6-1.5 L/min
Sample uptake rate	: 2 mL/min
Spectrometer	
Spectro Model : SPECTROFRAME EOP	
Monochromator 1	
Concave grating : 2400 grooves/mm, 120 nm-410 nm	
Focal length : 0.75 m	
Dispersion : 0.55 nm/mm at first order	
Mount : Paschen-Runge	
UV Optics : N_2 filled sealing with automatic purification system	
Direct wavelength drive method	
Monochromator 2	
Concave grating : 1200 grooves/mm, 260 nm-780 nm	
Mount : Paschen-Runge	
Detector : PMT	
Optical Plasma Interface for the axial viewing	
Sample introduction System	
Pneumatic Nebulizer : Concentric Nebulizer	
Ultrasonic Nebulizer : SPECTRO USN	
Torch : Semi-demountable	
Scott spray chamber	

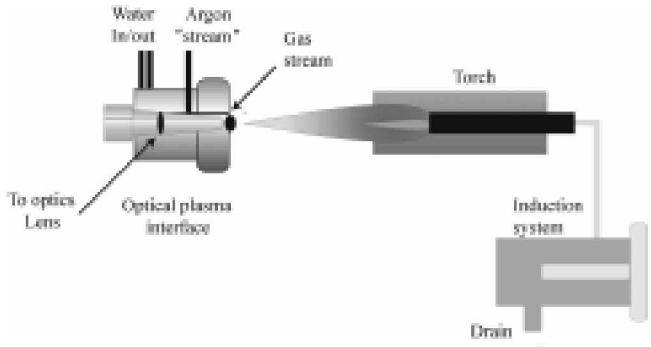

Figure 1. Schematic Diagram of Optical Plasma Interface (OPI) System (SPECTRO Analytical Instruments, with permission).

has been known to govern energy populations. For the measurement of excitation temperature, the relative intensities of two or more spectral lines of selected elements have been utilized.[3,4] In this work, the Fe I six-line set was selected for the estimation of excitation temperature. The selected wavelengths, the excitation energies, statistical weight of the emitting level, and relative transition probabilities for the excitation temperature calculation are described in Table 2.[3,4,7-13] The axial relative intensity profiles of the selected spectral lines for the Fe I analyte (a thermometric species) were obtained with E-O-V ICP-AES, then the following equation was used.

$$\ln (I_{pq}\lambda_{pq}/g_pA_{pq}) = -E_p/kT + \ln [nlhc/4\pi Z(T)] \quad (1)$$

Table 2. Fe Emission line data[3,4]

λ	E_p	g_{pq}	A_p
371.994	26875	11	0.163
373.487	33695	11	0.886
373.713	27167	9	0.143
374.826	27560	5	0.0904
374.949	34040	9	0.744
375.824	34329	7	0.611

Symbol used: λ = wavelength of the transition p → q; E_p = excitation energy of the emitting level; g_{pq} = statistical weight of the emitting level A_p = relative transition probabilities

I_{pq} = observed emission intensity
λ_{pq} = wavelength of the emission line
g_p = statistical weight of the level p
A_{pq} = transition probability for spontaneous emission
E_p = excitation energy of the level p
k = Boltzmann constant
T = temperature
n = total concentration of neutral atom or ion
l = path length of the source
h = Plancks constant
c = velocity of light
$Z(T)$ = partition function of atom or ion

T_{exc} is calculated from the slope of the straight line (−1/kT) fitted to a plot of the left-hand side of equation (1) against E_p.[3,4]

Measurement of Electron Number Density. In this work, the electron number densities were calculated from the Saha-Eggert ionization theory.[3,4,14-21] The used equation is described as follows:

$$n_e = 4.83 \times 10^{15} (J^0 g^+ A^- \lambda^- / J^+ g^0 A^0 \lambda^-) \times T^{3/2} \times \exp (E^+ - E^0 E^0_i - \Delta E^-_i / kT) \quad (2)$$

(0, +) = the neutral atom and singly ionized species, respectively
J = emission intensity
g = statistical weight of the emitting level
A = transition probability for spontaneous emission
λ = wavelength of the emission transition
T = excitation temperature
E = energy of the emitting level
E^0_i = ionization energy of the neutral atom species
ΔE^0_i = lowering of the ionization energy

The method requires relative emission intensities from the neutral atom and singly ionized species. The electron number densities were determined under the assumption that the plasma is in the local thermodynamic equilibrium (LTE) state.[3,4] An element of Fe with neutral atom ionization potential of 7.87 eV was selected for measurement of atom and ion emission lines intensities due to the sufficiently intense atom and ion spectral lines, availability of transition probability data, and freedom from spectral interferences. The wavelength lines for the selected atom and ion, stati-

Table 3. Emission line data for Saha-Eggert's Electron Number Density Calculations[3-4]

Species	λ (nm)	E_p	Average $(g^oA^o\lambda^+/g^+A^+\lambda^o)$ ratio
Fe I	252.285	39626	3.1354 ± 0.27
Fe II	258.558	38660	

symbols used: λ = wavelength of transition p → q; E_p = excitation energy of the emitting level

stical weights of emitting levels, and transition probability data are described in Table 3.[4]

Results and Discussion

Excitation temperature and electron number density with pneumatic nebulizer (PN). As we described in the experimental section, excitation temperatures were measured as a function of input power. The results are shown in Figure 2. As the excitation temperatures increased with the increasing power, the higher forwarded power input more energy into the plasma, resulting in the higher excitation temperature. The results were obtained with a solution of 10 μg/mL Fe at an injector gas flow rate of 1.0 L/min. The excitation temperatures ranged from 5700 K to 6000 K. The excitation temperatures for E-O-V ICP-AES were varied within the range of those for side-on view inductively coupled plasma atomic emission spectrometry (S-O-V ICP-AES).[3,4] Similarly, the electron number densities were measured at the different powers. As the results show in Figure 3, the electron number densities in the plasma, in general, also increased as the input power increased. The higher electron number densities might have resulted from the higher plasma temperatures. When other species (Ca and Mg) were investigated for electron number density,[4,14-21] the electron number density was generally lower compared with that obtained with Fe. In general, the excitation temperature and electron number density were higher at the higher power with pneumatic nebulizer. At any rates, the excitation temperatures and electron number densities for E-O-V ICP-AES were

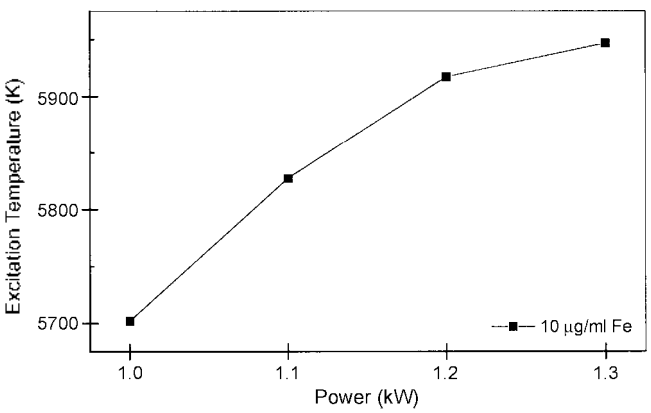

Figure 2. Excitation temperatures with PN (The concentration of Fe : 10 μg/mL).

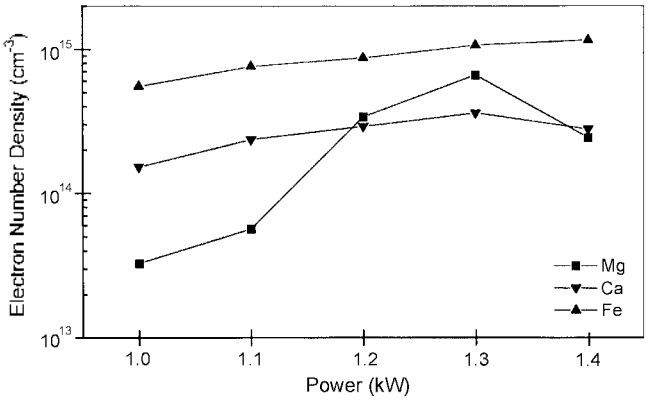

Figure 3. Electron number densities with PN (The concentration of Fe, Ca and Mg : 10 μg/mL).

almost the same as those for S-O-V ICP-AES.

The effect of Na on the excitation temperature and electron number density with PN. The excitation temperatures were measured with increasing concentration of Na. As the results show in Figure 4a, the highest excitation temperature was obtained at 1.3 kW. The plasma temperature at 1.4 kW was lower than that at 1.3 kW with this system because the coolant gas flow rate automatically increased as the power increased above 1.4 kW to prevent the torch from burning. This showed that the plasma temper-

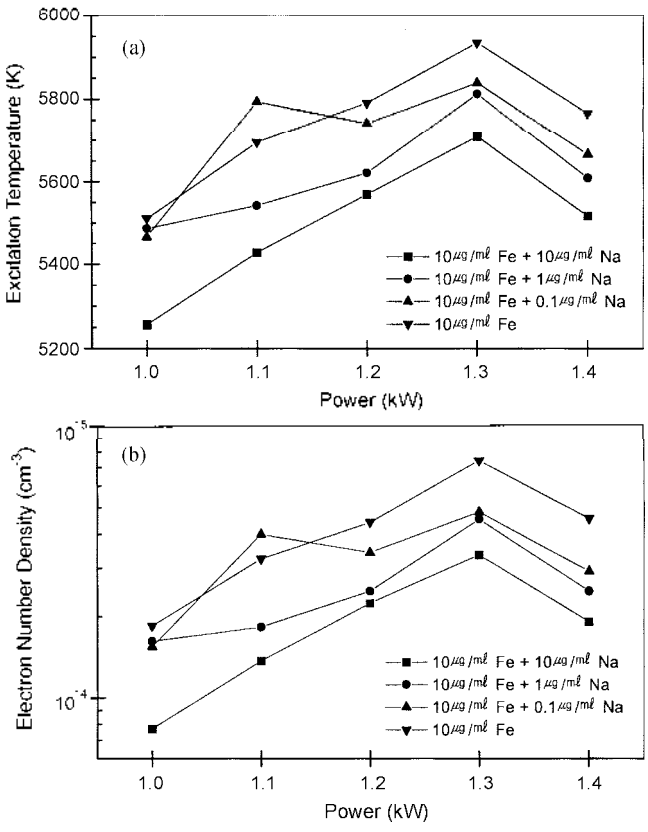

Figure 4. (a) Excitation temperatures of plasmas with and without Na element with PN. (b) Electron number densities of plasmas with and without Na element with PN.

ature decreased slightly as the concentration of Na increased in the sample. The excitation temperature of plasma was lowest when 10 μg/mL of sodium was added to the thermometric species of 10 μg/mL Fe. The results show that Na might cause the matrix effect. The electron number densities were also measured to investigate the effect of Na. As the results show in Figure 4b, the electron number densities also decreased with increasing Na. The decrease in electron number density might have resulted from the lower excitation temperature. The reason for the decrease in excitation temperature and electron number density could not be reasonably demonstrated. However, it shows that the emitting species in plasma could be interfered by the matrix element due to the space charge effect and ionization process. Thus, the decrease might be related to the matrix effect in elemental analysis.

The effect of the nebulizer gas flow rate on excitation temperature and electron number density with PN. The effect of the nebulizer gas flow rate for sample introduction on the excitation temperature and electron number density was investigated. As the results show in Figure 5a, the excitation temperature did not change for the range of nebulizer gas flow rate 0.83 L/min 1.05 L/min. But, the excitation temperature did decrease when the nebulizer gas flow rate increased from 1.05 L/min to 1.26 L/min. This might indicate that increasing gas into the plasma could result in cooling of the plasma. Figure 5b shows the effect of nebulizer gas flow on electron number density. As the results show, the electron number densities generally decreased with increasing rate of nebulizer gas flow. At 1200 W, the electron number densities were 2.50×10^{15}, 8.70×10^{14}, 2.25×10^{14} cm^{-3} at 0.83, 1.05, 1.26 L/min, respectively. As the temperature decreases with increasing gas flow, the electron number density might be reduced. The results show that the injector gas flow rate could influence the excitation temperature and electron number density, and affect the signals of elements in analysis. Thus, the injector gas flow rate should be well optimized for elemental analysis.

The effect of different nebulizers on excitation temperature and electron number density. The ultrasonic nebulizer (USN) was used for sample introduction instead of PN. The excitation temperature and electron number density with USN were measured and compared with those obtained with PN. As the results show in Figure 6a, the excitation temperatures of plasmas with USN were generally higher than those with PN. With USN, the lower loading of solvent in the plasma might be the reason for this. When USN was used for sample introduction, the sample aerosols produced by the transducer within USN were passed through the heating and cooling chamber to reduce the load of solvent into the plasma. The electron number densities with USN were also higher than those with PN. But, contrary to the results obtained by PN, the electron number densities increased with the increasing nebulizer gas flow rate. A logical explanation is not available. The measured electron number

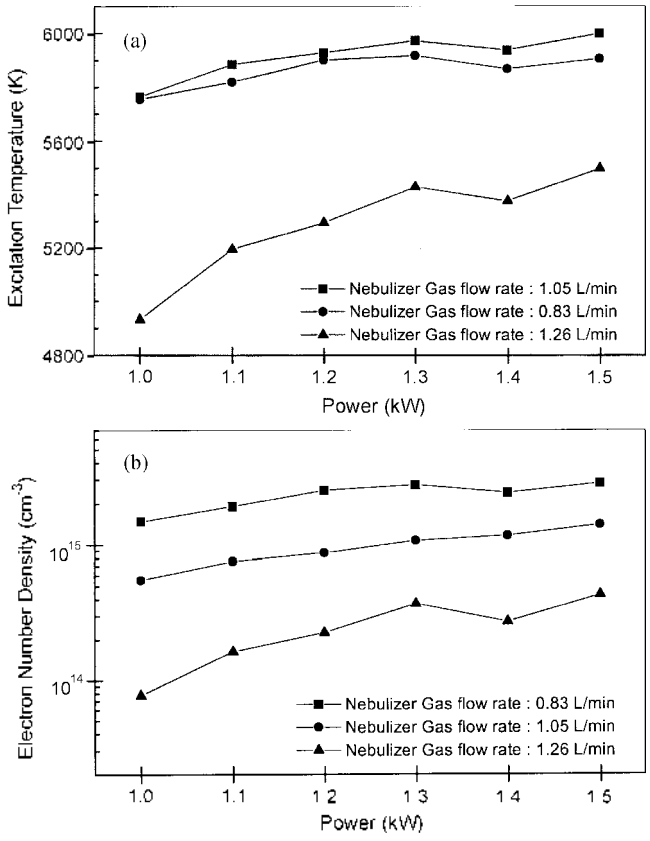

Figure 5. (a) Effect of different gas flow rate on excitation temperature of plasma with PN. (b) Effect of different gas flow rate on electron number density of plasma with PN.

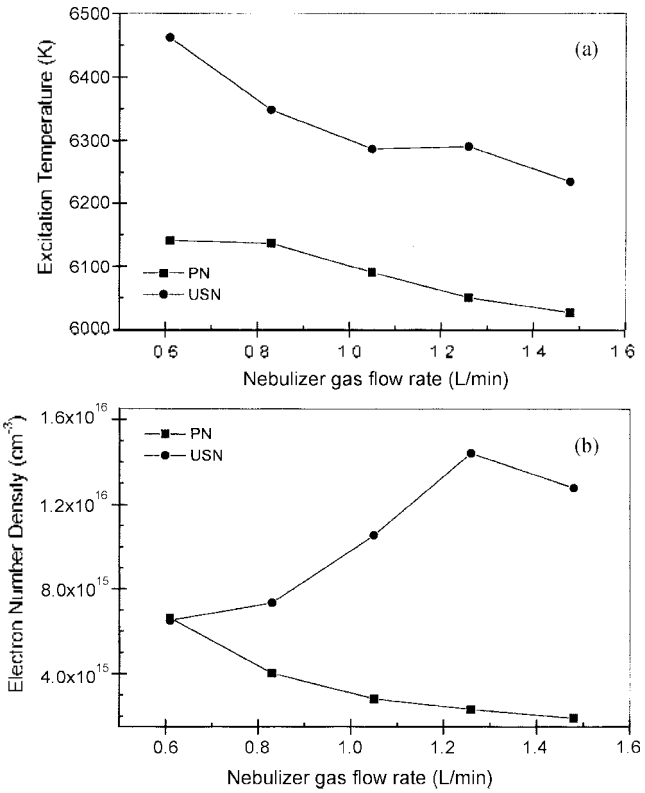

Figure 6. (a) Excitation temperatures of plasmas with PN and USN. (b) Electron number densities of plasmas with PN and USN.

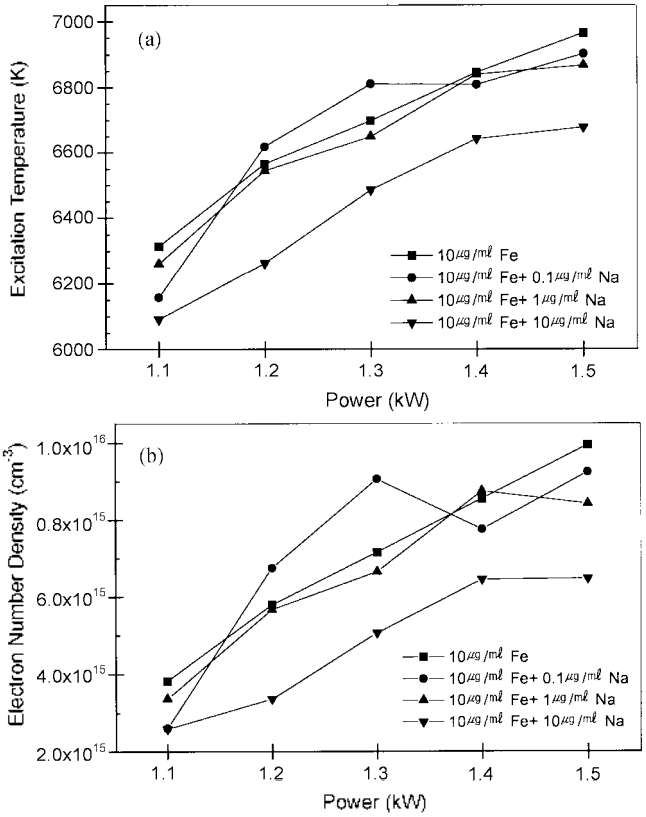

Figure 7. (a) Excitation temperatures of plasmas with and without Na element at USN. (b) Electron number densities of plasmas with and without Na element at USN

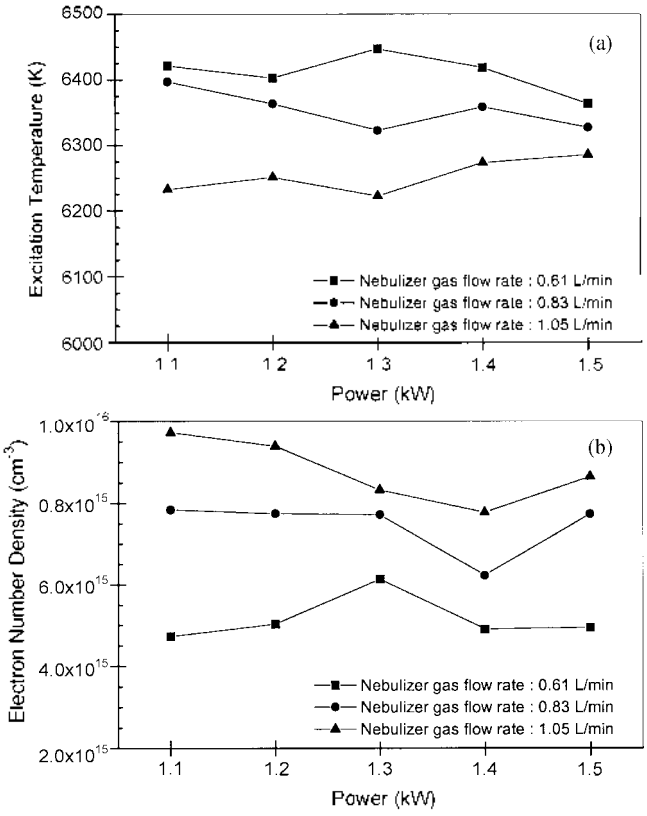

Figure 8. (a) Effect of different gas flow rate on excitation temperatures of plasmas with USN. (b) Effect of different gas flow rate on electron number densities of plasmas with USN.

densities with USN ranged from 6.4×10^{15} to 1.4×10^{16}cm^{-3} when the neublizer gas flow rates ranged from 0.6 to 1.5 L/min.

The effect of Na on excitation temperature and electron number density with USN. The excitation temperatures were measured with increasing concentration of Na. As the results show in Figure 7a, the lowest excitation temperatures were obtained when the Na added was 10 μg/mL. even though the excitation temperatures for 0.1 and 1 μg/mL Na were almost the same as those without Na. The electron number densities were also measured with USN while Na was added to the thermometric species of Fe. The results are described in Figure 7b. The trends were almost similar to those with the excitation temperatures with USN. The lowest electron number densities were obtained for 10 μg/mL Na added. The electron number densities ranged from 2.6×10^{15} to 1.0×10^{16} cm^{-3}. The results show that the high concentration of Na could interfere with the emitting species in plasma.

The effect of the nebulizer gas flow rate on the excitation temperature and electron number density with USN at different powers. The electron number densities and excitation temperatures were investigated at various nebulizer gas flow rates and powers with USN. The results for excitation temperature are shown in Figure 8a. The excitation temperatures slightly decreased with increasing nebulizer gas flow. but the excitation temperature did not change even when the powers were increased with fixed nebulizer gas flow rate. But, the electron number densities measured with USN increased with increasing nebulizer gas flow rate. even though the power did not affect the electron number densities in the plasma with USN.

Conclusions

The excitation temperatures measured for E-O-V ICP discharges were almost the same as those obtained with S-O-V ICP discharges. The excitation temperatures. in general. increased as the forwarded powers increased for E-O-V ICP discharges with PN. The excitation temperatures ranged from 5700 K to 6200 K with PN. The electron number densities for E-O-V ICP discharges were also similar to those with S-O-V ICP discharges with PN. Like the excitation temperature, the electron number densities generally increased as the input powers increased. The present study shows the concentration of Na in a sample can affect the excitation temperatures and electron number densities of plasmas. In general, the excitation temperatures and electron number densities decreased as the concentration of Na in the sample increased. This phenomenon might be related with matrix interference in elemental analysis. As the nebulizer gas flow rate increased. the excitation temperatures and electron number densities generally decreased with PN. The excitation temperatures and electron number densities obtained with USN

were higher than those with PN.

References

1. Montaser, A.; Golightly, D. W. *Inductively Coupled Plasma in Analytical Atomic Spectrometry*, 2nd ed; Wiley-VCH: New-York, 1992; pp 1-1017.
2. Boumans, P. W. *Inductively Coupled Plasma Emission Spetroscopy*, Part I & II; Wiley: New York, 1987.
3. Hasegawa, T.; Umemoto, M.; Haraguchi, H.; Hsiech, C.; Montaser, A. *Inductively Coupled Plasma in Analytical Atomic Spectrometry*, 2nd ed.; Montaser, A., Golightly, D. W., Eds.; Wiley-VCH: New York, 1992; ch 8, pp 373-449.
4. Kalnicky, D. J.; Fassel, V. A.; Kniseley R. N. *Appl. Spectrosc.* **1977**, *31*, 137.
5. Zahang, H.; Hsiech, C.; Ishii, I.; Zeng, Z.; Montaser, A. *Spectrochim. Acta* **1994**, *49B*, 817.
6. Iacone, L. I.; Masamba, W. R. L.; Nam, S.; Zhang, H.; Minnich, M. G.; Okino, A.; Montaser, A. *J. Anal. At. Spectrom.* **2000**, *15*, 419.
7. Eddy, T. L. *J. Quant. Spectrosc. Radiat. Transfer* **1985**, *33*, 197.
8. Huang, M.; Hieftje, G. M. *Spectrochim. Acta* **1985**, *40B*, 1387.
9. Marshall, K. A.; Hieftje, G. M. *Spectrochim. Acta* **1988**, *43B*, 841.
10. Scheeline, A.; Zoellner, M. *Appl. Spectrosc.* **1984**, *38*, 245.
11. Boumans, P. W. J. M.; DeBoer, F. J. *Spectrochim. Acta* **1977**, *31B*, 365.
12. Falk, H.; Hoffman, E.; Jaeckel, J.; Ludke, C. *Spectrochim. Acta* **1979**, *34B*, 333.
13. Houk, R. S.; Svec, H. J.; Fassel, V. A. *Appl. Spectrosc.* **1981**, *35*, 380.
14. Blades, M. W.; Caughlin, B. L. *Spectrochim. Acta* **1985**, *40B*, 579.
15. Olesik, J. W.; Den, S. J. *Spectrochim. Acta* **1990**, *45B*, 731.
16. Caughlin, B. L.; Blades, M. W. *Spectrochim. Acta* **1985**, *40B*, 987.
17. Furuta, T.; Nojiri, Y.; Fuwa, K. *Spectrochim. Acta* **1985**, *40B*, 423.
18. Huang, M.; Hieftje, G. M. *Spectrochim. Acta* **1989**, *44B*, 739.
19. Nowak, M.; Van Der Mullen, J. A. M.; Van Lammeren, A. C. A. P.; Schram, D. C. *Spectrochim. Acta* **1989**, *44B*, 411.
20. Walters, P. E.; Gunter, W. H.; Zeeman, P. B. *Spectrochim. Acta* **1986**, *41B*, 133.
21. Walters, P. E.; Barnardt, C. A. *Spectrochim. Acta* **1988**, *43B*, 325.
22. Dubuisson, C.; Poussel, E. *J. Anal. At. Spectrom.* **1997**, *12*, 281.
23. Conver, T. S.; Yang, J.; Koropchak, J. A.; Shkolnik, G.; Rivera, C. F. *Appl. Spectrosc.* **1997**, *51*, 68.
24. Ivaldi, J. C.; Tyson, J. F. *Spectrochim. Acta* **1995**, *Part B*, 1207.
25. Brenner, I. B.; Zander, A.; Cole, M.; Wiseman, A. *J. Anal. At. Spectrom.* **1997**, *12*, 897.
26. Todoli, J. L.; Mermet, J. M. *J. Anal. At. Spectrom.* **1998**, *13*, 727.
27. Gagean, M.; Mermet, J. M. *J. Anal. At. Spectrom.* **1997**, *12*, 198.
28. Skinner, C. D.; Salin, E. D. *J. Anal. At. Spectrom.* **1997**, *12*, 725.
29. Dubuisson, C.; Poussel, E.; Mermet, J. M. *J. Anal. At. Spectrom.* **1998**, *13*, 1265.
30. Dubuisson, C.; Poussel, E.; Mermet, J. M.; Todoli, J. L. *J. Anal. At. Spectrom.* **1998**, *13*, 63.
31. Nakamura, Y.; Takahashi, K.; Kufirai, O.; Okochi, H. *J. Anal. At. Spectrom.* **1997**, *12*, 349.
32. Tian, X.; Emteborg, H.; Adams, F. C. *J. Anal. At. Spectrom.* **1999**, *14*, 1807.
33. Tian, X.; Adams, F. C. *J. Anal. At. Spectrom.* **1999**, *14*, 1567.